



Understanding and overcoming fundamental limits of asymmetric light-light switches

SIMONE ZANOTTO,^{1,*} GIUSEPPE CARLO LA ROCCA,² AND ALESSANDRO TREDICUCCI^{3,4}

¹NEST, Istituto Nanoscienze - CNR and Scuola Normale Superiore, Piazza S. Silvestro 12, 56127 Pisa, Italy

²Scuola Normale Superiore and CNISM, Piazza dei Cavalieri 7, 56126 Pisa, Italy

³NEST, Istituto Nanoscienze - CNR, Piazza S. Silvestro 12, 56127 Pisa, Italy

⁴Dipartimento di Fisica “E. Fermi”, Università di Pisa, Largo Pontecorvo 3, 56127 Pisa, Italy

*simone.zanotto@nano.cnr.it

Abstract: The interplay between interference and absorption leads to interesting phenomena like coherent perfect absorption and coherent perfect transparency (CPA and CPT), which can be exploited for fully optical modulation. While it is known that it is possible to harness CPA and CPT for switching a strong signal beam with a weak control beam, it is not immediate that this process suffers from a fundamental compromise between the device efficiency (quantified by device loss and modulation depth) and the asymmetry between signal and control intensity desired for operation. This article quantifies this compromise and outlines a possible way to overcome it by means of a combination of optical gain and loss in the same photonic component. A general formulation and a specific device realization are both discussed.

© 2018 Optical Society of America under the terms of the [OSA Open Access Publishing Agreement](#)

OCIS codes: (260.3160) Interference; (130.4815) Optical switching devices; Gain-loss structures; Coherent absorption.

References and links

1. Y. D. Chong, L. Ge, H. Cao, and A. D. Stone, “Coherent perfect absorbers: Time-reversed lasers,” *Phys. Rev. Lett.* **105**, 053901 (2010).
2. W. Wan, Y. Chong, L. Ge, H. Noh, A. Stone, and H. Cao, “Time-reversed lasing and interferometric control of absorption,” *Science* **331**, 889 (2011).
3. D. G. Baranov, A. Krasnok, T. Shegai, A. Alù, and Y. Chong, “Coherent perfect absorbers: linear control of light with light,” *Nature Reviews Materials* **2**, 17064 (2017).
4. J. Yoon, K. H. Seol, S. H. Song, and R. Magnusson, “Critical coupling in dissipative surface-plasmon resonators with multiple ports,” *Opt. Express* **18**, 25702 (2010).
5. C. M. Bender and S. Boettcher, “Real Spectra in Non-Hermitian Hamiltonians Having PT-Symmetry,” *Phys. Rev. Lett.* **80**, 5243 (1998).
6. C. M. Bender, D. C. Brody, and H. F. Jones, “Complex extension of quantum mechanics,” *Phys. Rev. Lett.* **89**, 270401 (2002).
7. L. Ge, K. G. Makris, D. N. Christodoulides, and L. Feng, “Scattering in PT- and RT-symmetric multimode waveguides: Generalized conservation laws and spontaneous symmetry breaking,” *Phys. Rev. A* **92**, 062135 (2015).
8. L. Ge and L. Feng, “Optical-reciprocity-induced symmetry in photonic heterostructures and its manifestation in scattering PT-symmetry breaking,” *Phys. Rev. A* **94**, 043836 (2016).
9. L. Ge and L. Feng, “Contrasting eigenvalue and singular-value spectra for lasing and antilasing in a PT-symmetric periodic structure,” *Phys. Rev. A* **95**, 013813 (2017).
10. M. Lawrence, N. Xu, X. Zhang, L. Cong, J. Han, W. Zhang, and S. Zhang, “Manifestation of PT symmetry breaking in polarization space with terahertz metasurfaces,” *Phys. Rev. Lett.* **113**, 093901 (2014).
11. P. Ambichl, K. G. Makris, L. Ge, Y. Chong, A. D. Stone, and S. Rotter, “Breaking of PT symmetry in bounded and unbounded scattering systems,” *Phys. Rev. X* **3**, 041030 (2013).
12. V. Achilleos, G. Theoharis, O. Richoux, and V. Pagneux, “Non-hermitian acoustic metamaterials: Role of exceptional points in sound absorption,” *Phys. Rev. B* **95**, 144303 (2017).
13. S. Longhi, “PT-symmetric laser absorber,” *Phys. Rev. A* **82**, 031801 (2010).
14. Y. D. Chong, L. Ge, and A. D. Stone, “PT-symmetry breaking and laser-absorber modes in optical scattering systems,” *Phys. Rev. Lett.* **106**, 093902 (2011).
15. Z. J. Wong, Y.-L. Xu, J. Kim, K. O’Brien, Y. Wang, L. Feng, and X. Zhang, “Lasing and anti-lasing in a single cavity,” *Nature Photonics* **10**, 796 (2016).
16. Z. Lin, H. Ramezani, T. Eichelkraut, T. Kottos, H. Cao, and D. N. Christodoulides, “Unidirectional invisibility induced by PT-symmetric periodic structures,” *Phys. Rev. Lett.* **106**, 213901 (2011).

17. J.-H. Wu, M. Artoni, and G. C. La Rocca, "Non-hermitian degeneracies and unidirectional reflectionless atomic lattices," *Phys. Rev. Lett.* **113**, 123004 (2014).
18. J.-H. Wu, M. Artoni, and G. C. La Rocca, "Coherent perfect absorption in one-sided reflectionless media," *Scientific Reports* **6**, 35356 (2016).
19. L. Feng, Y.-L. Xu, W. S. Fegadolli, M.-H. Lu, J. E. B. Oliveira, V. R. Almeida, Y.-F. Chen, and A. Scherer, "Experimental demonstration of a unidirectional reflectionless parity-time metamaterial at optical frequencies," *Nature Materials* **12**, 108 (2012).
20. A. Regensburger, C. Bersch, M.-A. Miri, G. Onishchukov, D. N. Christodoulides, and U. Peschel, "Parity-time synthetic photonic lattices," *Nature* **488**, 167 (2012).
21. W. Wang, L.-Q. Wang, R.-D. Xue, H.-L. Chen, R.-P. Guo, Y. Liu, and J. Chen, "Unidirectional excitation of radiative-loss-free surface plasmon polaritons in PT-symmetric systems," *Phys. Rev. Lett.* **119**, 077401 (2017).
22. G. C. R. Devarapu and S. Foteinopoulou, "Broadband near-unidirectional absorption enabled by phonon-polariton resonances in SiC micropillar arrays," *Phys. Rev. Applied* **7**, 034001 (2017).
23. T. Roger, S. Vezzoli, E. Bolduc, J. Valente, J. J. F. Heitz, J. Jeffers, C. Soci, J. Leach, C. Couteau, N. I. Zheludev, and D. Faccio, "Coherent perfect absorption in deeply subwavelength films in the single-photon regime," *Nature Communications* **6**, 7031 (2015).
24. S. M. Barnett, J. Jeffers, A. Gatti, and R. Loudon, "Quantum optics of lossy beam splitters," *Phys. Rev. A* **57**, 2134 (1998).
25. S. Huang and G. S. Agarwal, "Coherent perfect absorption of path entangled single photons," *Opt. Express* **22**, 20936 (2014).
26. H. Zhao, W. Fegadolli, J. Yu, Z. Zhang, L. Ge, A. Scherer, and L. Feng, "Metawaveguide for asymmetric interferometric light-light switching," *Phys. Rev. Lett.* **117**, 193901 (2016).
27. L. Baldacci, S. Zanotto, G. Biasiol, L. Sorba, and A. Tredicucci, "Interferometric control of absorption in thin plasmonic metamaterials: general two port theory and broadband operation," *Opt. Express* **23**, 9202 (2015).
28. S. Xiao, V. P. Drachev, A. V. Kildishev, X. Ni, U. K. Chettiar, H.-K. Yuan, and V. M. Shalaev, "Loss-free and active optical negative-index metamaterials," *Nature* **466**, 735 (2010).
29. S. Wuestner, A. Pusch, K. L. Tsakmakidis, J. M. Hamm, and O. Hess, "Overcoming losses with gain in a negative refractive index metamaterial," *Phys. Rev. Lett.* **105**, 127401 (2010).

1. Introduction

Linear wave optics phenomena, despite being a direct consequence of Maxwell's equations, are still at the focus of active research, thanks to the emergence of novel features having both fundamental character and applicative interest. Photonic crystals, metamaterials, light transport in complex environments, and plasmonics are widely investigated; with these concepts it is now possible to manipulate light in an unconventional way and to confine it at the nanoscale level, opening new avenues for sensing, energy handling, and information control.

More recently, peculiar phenomena have been reported when a linear optical system features an appropriate distribution of gain, loss and excitation field. A lossy system can exhibit coherent perfect absorption (CPA) [1–3], basically an extension of critical coupling to multiport systems [4], where all the incident energy from a tailored field distribution is absorbed as in a sort of "anti-laser". Following insights from researches in the foundations of quantum mechanics [5, 6], it has been observed that by introducing gain elements such that the optical device follows the parity-time (PT) symmetry, a phase transition occurs, dividing regions where the device operation is unitary from others where it is not [7–12]. In particular, a class of PT-symmetric systems can switch from CPA to lasing through an appropriate tuning of input fields [13–15]. Moreover, PT-symmetric systems support unidirectional modes which can be exploited for asymmetric - yet reciprocal - devices [16–21] which go beyond the capabilities of asymmetric structures with pure losses [22].

These phenomena can form the heart of advanced signal processing techniques, where an optical beam can be fully controlled by a second one, possibly down to the single photon level [23–25]. In particular it has been proposed that CPA in an asymmetric metawaveguide, whose design is inspired by the PT symmetry concept, can be exploited for linear light-light switching of an intense beam with a much weaker one, with clear implications for optical information technology [26]. The focus of the present article is to provide a deeper understanding of CPA-based devices for asymmetric optical control, highlighting a fundamental limitation

which makes it impossible to build a device where a weak beam perfectly switches on and off an intense beam. The limitation stems from energy conservation considerations and is hence of extremely wide validity; indeed, it applies to every two-port light-light switch constituted of passive optical materials. Analysis based on singular value decomposition provides a global picture of the phenomenon and allows for a quantification of extinction ratios and insertion losses. It will then be shown that lifting the assumption that the device only contains passive optical materials makes it possible to conceive a perfect asymmetric light-light switch. Finally, a prototypical yet realistic device, based on Fabry-Pérot resonances in a gain-loss slab, will be proposed as an implementation of the perfect asymmetric switch. Incidentally, the operating points of this system turn out to be arranged in a surprisingly rich structure, despite its apparent simplicity.

2. Fundamental limits of asymmetric light-light switches

The main argument about fundamental limitations stems from applying energy conservation to the formalism that some of us reported in [27] and from its geometrical interpretation, which we recall for clarity. The linear optical response of a two-port system is described by the scattering matrix S , which connects the input amplitudes to the output amplitudes: $(s_1^-, s_2^-)^t = S(s_1^+, s_2^+)^t$. Here, labels 1 and 2 refer to the ports, and $+$, $-$ refer to incoming and outgoing waves, respectively.

Thus, $S = \begin{pmatrix} r_1 & t \\ t & r_2 \end{pmatrix}$, being r the reflectivities and t the transmissivity (reciprocity is assumed).

Having then defined the single-beam absorbances $A_{1,2} = 1 - |r_{1,2}|^2 - |t|^2$ and the modulating absorbance $A_{\text{mod}} = \sqrt{(1 - A_1)(1 - A_2) - |\det S|^2}$, the total output intensity $I_{\text{out}} = |s_1^-|^2 + |s_2^-|^2$ is

$$I_{\text{out}} = 1 - \frac{1+x}{2}A_1 - \frac{1-x}{2}A_2 + \sqrt{1-x^2} A_{\text{mod}} \sin(\gamma + \delta) \quad (1)$$

where $\gamma = \arg(s_2^+/s_1^+)$ is the phase difference between input beams, δ is a function of the S -matrix elements, and $x = |s_1^+|^2 - |s_2^+|^2$ is the difference in the beam intensities, i.e., the unbalance between “control” and “signal” beams. Here we assume that the total input intensity is unity. The total output intensity I_{out} attains minimum and maximum values when the relative input beam phase γ assumes appropriate values. We will refer to the minimum and maximum values of I_{out} as $I_{\text{out,off/on}}$, recalling the application to optical switches. What is relevant for the purpose of this work is that $I_{\text{out,off/on}}(x)$ describes an ellipse in the $x - I_{\text{out}}$ plane, and that the ellipse is bound by the condition $0 \leq I_{\text{out}} \leq 1$, which evidently holds for systems where energy is conserved, i.e., for passive systems.

To fix the notation, in this article we assume that beam 1 is the strong signal and beam 2 is the weak control; at the operating point, x assumes a value close to +1 which we label \bar{x} . In other words, with obvious notation, $\bar{x} = I_{\text{in}}^{\text{sig}} - I_{\text{in}}^{\text{contr}}$. A possible desired configuration is that of having CPA at \bar{x} , like in Figs. 1(a) and 1(c); this is possible by a proper tailoring of the S -matrix. To maximize the modulation depth, the S -matrix needs to be further adjusted in order to have the largest possible $I_{\text{out,on}}(\bar{x}) - I_{\text{out,off}}(\bar{x})$: it is immediate to see that this occurs when the ellipse is fully enlarged such that $I_{\text{out,on}}(-\bar{x}) = 1$. In other words, the system must also have the possibility to show CPT (*coherent perfect transparency*). Unfortunately, it is *not possible* to have access to both CPA and CPT simultaneously, in the sense that a simple manipulation of the relative phase γ between signal and control beams is not able to connect CPA and CPT points. Rather, the phase sweep links the CPA condition to a weaker *coherent transparency* (CT) condition, where the intense signal beam is only partially transmitted.

Following the above observations, another possibility for extremal, yet non-optimal, asymmetric light-light switching appears. This is simply the system symmetrical to that considered above: its coherent absorption ellipse is that of Fig. 1(d). Now, the phase sweep allows to pass from the CPT condition to a *coherent absorption* (CA) condition. Notice that here the coherent perfect

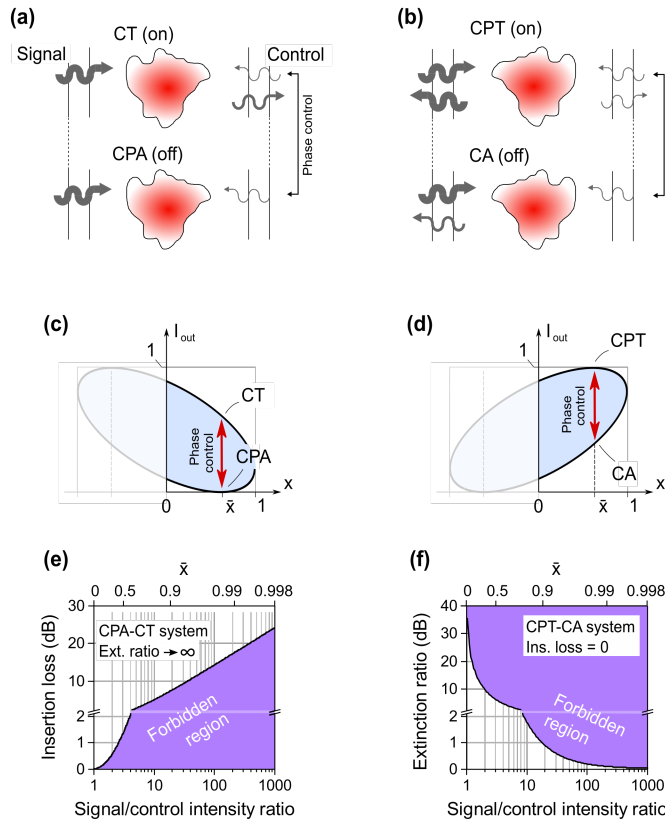


Fig. 1. Panels (a)-(f), fundamental limitations of asymmetrical light-light switching devices based on engineered losses. In a system implementing CT and CPA (coherent transparency and coherent perfect absorption), panel (a), a strong signal can be completely stopped by a weak control. Acting on the phase of the control beam, the signal can be allowed to partially pass through the device, without however reaching full transparency. The limitation is dictated by the constraints on the absorption modulation ellipse, represented in panel (c) for the CT-CPA case. The intensity asymmetry between signal and control at the operating point is $\bar{x} = I_{in}^{sig} / I_{in}^{contr}$, assuming $I_{in}^{sig} + I_{in}^{contr} = 1$. Panel (e) reports the insertion loss - i.e., the penalty on the output intensity at CT - that a CPA-CT device must undergo. Panels (b, d, f), analogous constraints for a CPT-CA (coherent perfect transparency/coherent absorption) light-light switch. In this configuration there is no insertion loss (i.e., the signal does not get absorbed in CPT), but there is a finite extinction ratio (i.e., the signal does not reach zero at CA).

transparency has to be interpreted in the generalized sense introduced in [27]: *transparency* means that the system is *not absorbing any of the input light*, not that a beam (the signal beam) is actually *perfectly transmitted straight-through the structure*. It will indeed be shown in the following that a system described by the ellipse of Fig. 1(d) behaves as in Fig. 1(b): at CPT the signal beam is perfectly reflected, while when CA is reached the signal gets partially absorbed.

This behaviour follows directly from the S -matrix form that a system must have to implement the above conditions. The key is to consider the singular value decomposition (SVD) of S . Following [9], the squared singular values of S are the extremal values that the output intensity can reach, as the unit norm input vector (s_1^+, s_2^+) is varied. The SVD is written as $S = U\Sigma V^\dagger$, where Σ is a diagonal matrix whose entries are the singular values σ_i , while U and V are unitary

matrices whose columns, respectively $|\Phi_i\rangle$ and $|\Psi_i\rangle$, are the left and right singular vectors of S . They get mapped into each other by S , following $S|\Psi_i\rangle = \sigma_i|\Phi_i\rangle$ and $\langle\Phi_i|S = \langle\Psi_i|\sigma_i$. Here we construct the most general S for a reciprocal passive 2-port system which features CPA and CPT. Reciprocity implies $S = S^t$, hence $V = \bar{U}$ (here the bar stands for the element by element complex conjugation) and $S = U\Sigma U^t$. From the ellipse picture, it is evident that CPA and CPT are the extrema of the output intensity, hence the two singular values must be $\sigma_{\text{CPT}} = 1$ and $\sigma_{\text{CPA}} = 0$. U is an arbitrary 2×2 unitary matrix, a possible parametrization of which is the following:

$$U = e^{i\phi/2} \begin{pmatrix} e^{i\phi_1} \cos \theta & e^{i\phi_2} \sin \theta \\ -e^{-i\phi_2} \sin \theta & e^{-i\phi_1} \cos \theta \end{pmatrix}. \quad (2)$$

Thus,

$$S = e^{i\phi} \begin{pmatrix} e^{2i\phi_1} \cos^2 \theta & -e^{i(\phi_1-\phi_2)} \cos \theta \sin \theta \\ -e^{i(\phi_1-\phi_2)} \cos \theta \sin \theta & e^{-2i\phi_2} \sin^2 \theta \end{pmatrix}. \quad (3)$$

The first and second columns of \bar{U} constitute respectively the vectors $|\Psi_{\text{CPT}}\rangle$ and $|\Psi_{\text{CPA}}\rangle$, i.e., the input vectors which correspond to CPT and CPA. The input vectors corresponding to CA and CT are instead, respectively, $|\tilde{\Psi}_{\text{CPT}}\rangle$ and $|\tilde{\Psi}_{\text{CPA}}\rangle$, constructed imposing a π -phase shift of the second beam: $|\tilde{\Psi}\rangle = \begin{pmatrix} 1 & 0 \\ 0 & -1 \end{pmatrix} |\Psi\rangle$. Assuming that beam 1 is the signal and beam 2 the control,

to work with the CPA-CT system [Fig. 1(a) and 1(c)] one must choose $\sin^2 \theta - \cos^2 \theta = \bar{x}$, or, in other words, $\sin^2 \theta / \cos^2 \theta = I_{\text{in}}^{\text{sig}} / I_{\text{in}}^{\text{contr}}$. Notice that, since $I_{\text{in}}^{\text{sig}} / I_{\text{in}}^{\text{contr}} \gg 1$, $|\sin \theta| \gg |\cos \theta|$. Analyzing the output phases and amplitudes leads to the diagram of Fig. 1(a), where beams with amplitudes of the order $\cos^2 \theta$ have been neglected. Similarly, to work with the CPT-CA system the condition is $\cos^2 \theta - \sin^2 \theta = \bar{x}$; this leads to the amplitudes and phases of Fig. 1(b), where now beams with amplitudes of the order of $\sin^2 \theta \ll 1$ have been neglected.

The above formulation allows for a direct and quantitative analysis of the compromise between the requirements of strong signal/control asymmetry and of effective switching operation. For switching devices, effectiveness is usually quantified through two parameters, extinction ratio and insertion loss, respectively defined in dB scale as $\text{ER} = 10 \log_{10} I_{\text{out,on}} / I_{\text{out,off}}$ and $\text{IL} = -10 \log_{10} I_{\text{out,on}}$. Let's first analyze the CPA-CT system. Here one has always an ideal $\text{ER} \rightarrow \infty$, while the IL is limited by $I_{\text{out,on}} \leq 1 - \bar{x}^2$. This behavior is depicted in Fig. 1(e), where it can be noticed that, for a quite small signal/control intensity ratio of 10, a large IL of about 5 dB has to be borne at least. If larger values of $I_{\text{in}}^{\text{sig}} / I_{\text{in}}^{\text{contr}}$ are required, the device will introduce huge losses of several tens of dB. Analogously, in the CPT-CA system, the ideal behavior of the insertion loss ($\text{IL} = 0$) is counterbalanced by a penalty on the extinction ratio, which is bound from above by the fact that $I_{\text{out,off}} \geq \bar{x}^2$ [Fig. 1(f)]. Here, when $I_{\text{in}}^{\text{sig}} / I_{\text{in}}^{\text{contr}} = 10$, a tiny ER of about 1.7 dB can be achieved at best; larger values of $I_{\text{in}}^{\text{sig}} / I_{\text{in}}^{\text{contr}}$ imply a decrease of ER even to sub-dB levels. In essence, asymmetric light-light switching by means of passive absorptive interferometric devices becomes rapidly impractical as reasonable signal/control ratios are to be handled.

3. Overcoming the fundamental limits by gain-loss structures

Leveraging on the picture of CPA-CPT physics discussed hereby, it can be easily recognized that the limitations on asymmetric light-light switching can be overcome relying on hybrid loss-gain structures. For such a compound structure, the coherent absorption ellipse is no more bound by $I_{\text{out}} \leq 1$, and a situation like that in Fig. 2 can be envisaged. Now, the system operates as a true perfect asymmetric switch, where acting on the phase of a weak control implies a full switching of the strong signal. Notice that now the signal beam either is stopped or it passes straight through the two-port system. This feature is a consequence of the S -matrix form that an asymmetric CPA-CPT system must fulfil. Such form follows from $S|\Psi\rangle = 0$ and $|S|\tilde{\Psi}\rangle|^2 = |\tilde{\Psi}\rangle|^2$,

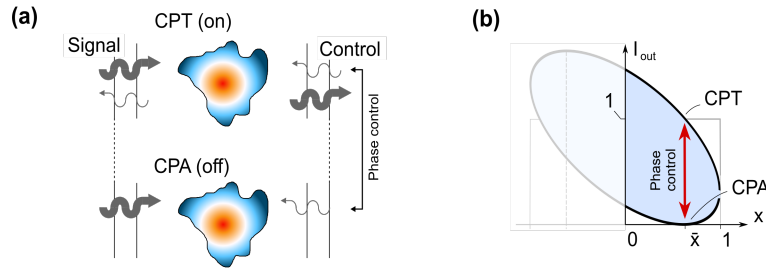


Fig. 2. Concept of perfect asymmetric light-light switch in a CPA-CPT (coherent perfect absorption/transparency) device. By acting on the phase of a weak control beam it is possible to completely turn on and off an arbitrarily intense beam. The system must include a gain element: to have CPA and CPT at an operating intensity difference $\bar{x} = I_{\text{in}}^{\text{sig}} - I_{\text{in}}^{\text{contr}} \neq 0$ the coherent modulation ellipse must allow for output intensities exceeding unity (when input intensity is normalized to one, $I_{\text{in}}^{\text{sig}} + I_{\text{in}}^{\text{contr}} = 1$).

where, as above, the tilde operator switches the relative phase of the vector components by π , and $|\Psi\rangle = (\sqrt{I_{\text{in}}^{\text{sig}}}e^{i\zeta}, \sqrt{I_{\text{in}}^{\text{contr}}})$ is the most generic input vector with the appropriate ratio between signal and control. Straightforward algebra leads to

$$S = \frac{e^{i\phi}}{2} \begin{pmatrix} -\sqrt{\frac{I_{\text{in}}^{\text{contr}}}{I_{\text{in}}^{\text{sig}}}}e^{-i\zeta} & 1 \\ 1 & -\sqrt{\frac{I_{\text{in}}^{\text{sig}}}{I_{\text{in}}^{\text{contr}}}}e^{i\zeta} \end{pmatrix} \quad (4)$$

which implies the amplitude and phase relations sketched in Fig. 2(a). Notably, it results that the very same system which acts as a perfect CPA-CPT switch when one port is illuminated by a strong signal and the other by a weak probe exhibits a radically different behaviour if the role of the ports is reversed: indeed, the system will act as a strong amplifier, with an output intensity (upon unity total input intensity) equal to the square of the larger singular value of S .

This amounts to $\left(\sqrt{I_{\text{in}}^{\text{sig}}/I_{\text{in}}^{\text{contr}}} + \sqrt{I_{\text{in}}^{\text{contr}}/I_{\text{in}}^{\text{sig}}}\right)^2/4$, which diverges as $I_{\text{in}}^{\text{contr}}/I_{\text{in}}^{\text{sig}} \rightarrow \infty$.

4. A prototype perfect asymmetric light-light switch

Having developed the general theory of asymmetric CPA-CPT, we will now analyze a prototypical yet realistic system capable of this operation. The device is schematized in Fig. 3(a): it consists of two dielectric layers, with complex refractive indices $n_{1,2} \pm ik_{1,2}$. n_i and k_i are positive quantities, hence layer 1 has losses and layer 2 has gain, assuming an $\exp(-i\omega t)$ dependence for the time-harmonic fields. In the illustration, the position of the loss layer towards the signal side is not casual, as it can be shown that it is impossible to find solutions to the problem if the loss layer is placed to the side of the weak control beam. This system can be practically implemented using polymeric thin-film techniques, where doping with nanoparticles and/or dyes in conjunction with appropriate pumping schemes can provide the required tuning of the complex refractive index profile [28, 29]. The scattering matrix of this bilayer can be expressed in closed form, and it depends on six real parameters: $n_{1,2}$, $k_{1,2}$, and $L_{1,2}/\lambda$, where λ is the vacuum wavelength. In the following, for simplicity, we will assume $\lambda = 1$, and thus write L_i instead of L_i/λ . We look for an S matching the form (4) by means of a numerical approach. Here we analyze the solutions obtained fixing $n_1 = n_2 = 1.5$. In a first step we looked for solutions with $I_{\text{in}}^{\text{sig}}/I_{\text{in}}^{\text{contr}} = 60$. The

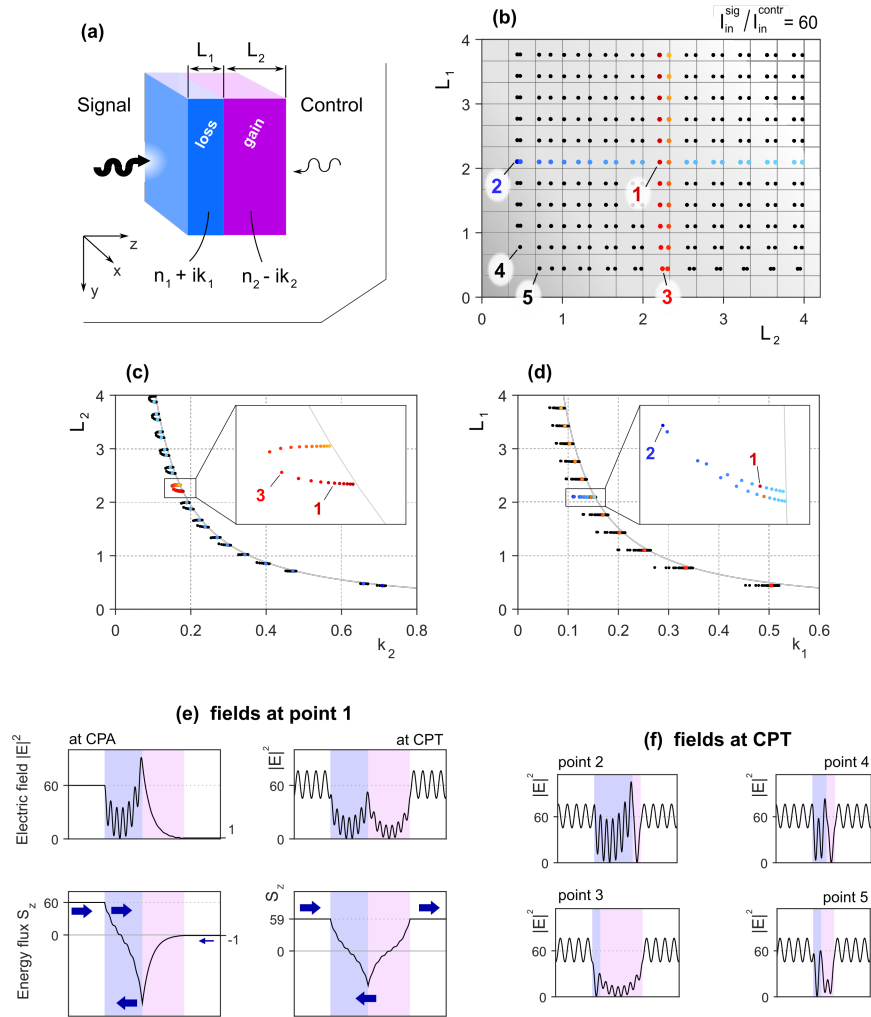


Fig. 3. A minimal implementation of a CPA-CPT device, consisting of a gain/loss bilayer slab (a). To fulfil the CPA-CPT conditions, appropriate conditions on the refractive indices $n_1 + ik_1, n_2 - ik_2$ and on the thicknesses $L_{1,2}$ are required. Panel (b) reports the L_1, L_2 pairs that satisfy the CPA-CPT condition, assuming $n_1 = n_2 = 1.5$ and signal/control intensity ratio equal to 60. The grid lines represent the Fabry-Pérot conditions for the two slabs. Panels (c-d), projection of the solution set on the $k_1 - L_1$ and $k_2 - L_2$ planes. Some points are colored to help the matching with the representation on the $L_1 - L_2$ plane. The solid lines are power-laws towards which solutions accumulate. Panels in (e), fields in the structure corresponding to point 1. Input phases fulfilling CPT and CPA are imposed; intensity ratio is 60:1. Units are chosen such that the Poynting vector has the same magnitude as the squared electric field. Panels in (f), comparison of CPT fields for different structures. The number of field minima in the gain/loss layers correspond to the Fabry-Pérot order observed in (b).

solutions are summarized in Fig. 3(b)-3(d): each point in the graphs corresponds to a single set (k_1, k_2, L_1, L_2) which satisfy Eq. (4). The solutions fill the parameter space in a complex but structured fashion, partly following common physical insight and partly developing curious patterns. Consider for instance Fig. 3(b), where the solutions have been projected on the (L_2, L_1) plane. A series of Fabry-Pérot-like structures appear, still with two main deviations from the ordinary behaviour. By comparing the solutions with the grid in the figure (which marks the usual conditions of resonance for each slab), it can be noticed that on the L_2 axis the actual free spectral range (FSR) is half that of an ordinary Fabry-Pérot. Half of the solutions are close to the resonance condition $L_2 = m_2/2n_2$ (m_2 being an integer), while the other half lie between two consecutive resonances. This behaviour is reminiscent, although going in the opposite direction, of the FSR doubling phenomenon observed in CPA-laser systems [14]. On the contrary, the distribution of solutions along the L_1 axis follows the Fabry-Pérot FSR, although the points are systematically offset by a fraction of the FSR. Consider now Fig. 3(c)-3(d), where the solution sets are projected on the (k_i, L_i) planes. The solution points cluster in manifolds, which globally follow a power-law distribution highlighted by the grey curve. This power law is similar, but not equal to the one that would follow from a constant absorption (constant gain) argument, i.e., $k_i L_i = \text{const}$. Rather, one has $L_1 = 0.213 k_1^{-1.22}$ and $L_2 = 0.305 k_2^{-1.15}$. It is also interesting to notice the correspondence between the solution manifolds among the different projections. For instance, the points highlighted in red hues, which belong to one FSR of L_2 , are mapped into one “pocket” on the (k_2, L_2) plane. A similar behaviour is observed about the resonances belonging to one FSR of L_1 (blue hue points), although here the pocket has a sharper shape. In light of these observations, it turns out that the points which in the (k_1, L_1) plane accumulate towards the power law curve are those corresponding to large L_2 (and small k_2), i.e., to perturbative solutions for the gain layer. Symmetrically, the points which in the (k_2, L_2) plane accumulate towards the power law curve are those corresponding to large L_1 , i.e., to perturbative solutions for the loss layer. It should be recalled that the points in Fig. 3(b)-3(d) are solutions to the CPA-CPT problem in the sense that the system’s S -matrix satisfies Eq. (4) with a given $I_{\text{in}}^{\text{sig}}/I_{\text{in}}^{\text{contr}}$ but with no requirements on ϕ and ζ . However, each solution in Fig. 3(b)-3(d) has its own ϕ and ζ (not plotted), and it can be shown that the role of ζ is connected to the presence of two solutions per FSR. Numerical analysis reveals that, in the limit of large L_1 , these two solutions have the same S -matrix except for a difference of π between the values of ζ . In other words, the two solutions are odd and even solutions, as the value of ζ dictates the phase relations between input and output signal and control beams at CPA-CPT.

As the main aim of the present article is to investigate (strongly) asymmetric light-light switching, we now focus on the role of signal/control intensity ratio in the loss-gain bilayer slab. The key point is here whether it is possible to find a S -matrix of the form (4) for arbitrary ratios $I_{\text{in}}^{\text{sig}}/I_{\text{in}}^{\text{contr}}$, and which is the structure of the corresponding solutions. Detailed analysis reveals that the requirement of larger signal/control intensity ratios leads to a narrowing of the solution set: in essence, the solutions do not fill any more the (L_1, L_2) plane, as low-order solutions are no more admitted. The narrowing of solution space ends up eventually in the impossibility to find any solution, and asymmetries larger than ≈ 150 are out of reach. The effect of requiring larger signal/control ratios is evidenced in Fig. 4, where the solutions are projected on the plane $(k_1 L_1, k_2 L_2)$. In this representation, the solutions for a given value of $I_{\text{in}}^{\text{sig}}/I_{\text{in}}^{\text{contr}}$ cluster into a spike-like arrangement, with “fibers” corresponding to the Fabry-Pérot resonance families previously described. It is interesting to compare the solution clusters with the line $k_1 L_1 = k_2 L_2$, which describes balanced losses and gain in a single-pass framework. The upper region of each cluster is constituted by an accumulation of points linked by $k_1 L_1 = k_2 L_2 + \text{const}$, where the constant depends on the signal/control asymmetry. As anticipated above, getting close to intensity ratios of ≈ 140 implies an evident narrowing of the solution set, which nonetheless mostly preserves the overall structure.

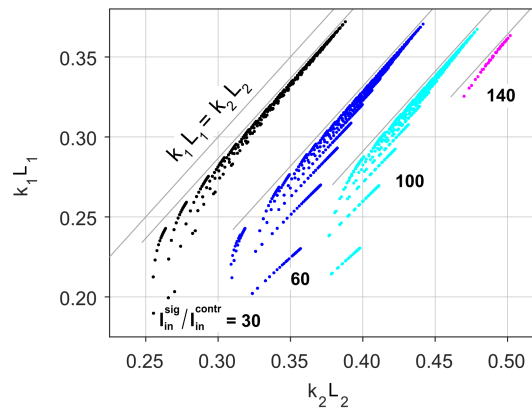


Fig. 4. Solution clusters corresponding to different signal/control ratios, represented on the $(k_1 L_1, k_2 L_2)$ plane. Each “fiber” of the cluster corresponds to a Fabry-Pérot family, i.e., to groups such as the colored sets in Fig. 3(b). The cluster cutoffs at large $k_1 L_1$ are due to the finite extension of the numerical space search.

5. Conclusion

In conclusion we have identified a fundamental limitation for light-light switches where a weak control interferometrically modulates an intense signal beam. This class of devices suffers from finite insertion losses or imperfect extinction ratios, that become more severe as stronger requirements on the signal-control asymmetry are asked for. This poses a limitation to the potential applications to actual optical signal processing systems. Nonetheless, the limitation can be overcome by relaxing one of the assumptions usually made, i.e., the passiveness of the device. Allowing for the presence of gain, perfect switching of a strong signal by a weak control can be attained, when the appropriate coherent perfect absorption – coherent perfect transparency (CPA-CPT) condition is met. This condition is simply expressed in terms of the scattering matrix and can be virtually implemented in a multitude of systems, either based on optical fiber, integrated photonics, photonic crystals, plasmonics, metamaterials or simply multilayer technologies. The latter approach has been analyzed in detail, revealing a series of possible parameter configurations required for a perfect asymmetric light-light switch. Moreover, the structure of the solution shows an interest *per se*, as it displays curious arrangements and clustering in the parameter space, unexpected from a system as simple as this, and going beyond basic physical considerations.

Funding

European Research Council (ERC-FP7-321122 SouLMan).

Acknowledgments

The authors acknowledge insightful discussions with Lorenzo Baldacci, Dr. Alessandro Pitanti, and Prof. Hui Cao.